Numerical Borehole Tensorial gravity modelling and its Implication

Damera Hima Vamshee [1] *and Ramabhatlla G. Sastry*[2,*]

1. *Department of Earth Sciences, IIT Roorkee, Roorkee* vamsheefly@gmail.com

2. School of Earth, Ocean and Climate Sciences, IIT Bhubaneswar, Bhubaneswar rgsastry@iitbbs.ac.in / rgssastry@gmail.com

**Corresponding author*

Key Words: Borehole Tensorial gravity, arbitrarily oriented parallelepiped, Forward problem

Summary

The characterization of fractured reservoirs is a challenging problem. Generally, surface seismic data is utilized in such cases. However, for deep-seated targets, this method can't provide high-resolution images of the subsurface. By considering recent advances in tensorial gravity, we wish to explore the feasibility of gravity gradiometry in boreholes to delineate the fractures containing hydrocarbon reserves in carbonate reservoirs. Here, we propose a novel transformation matrix, which helps in generating the tensorial gravity responses for an arbitrarily oriented rectangular parallelepiped. We use these synthetic forward responses to create tensorial gravity logs in different boreholes with respect to the buried model and analyze them for model parameters. Our theoretical formulations for synthetic tensorial gravity responses of an arbitrarily oriented rectangular parallelepiped open up new possibilities for borehole tensorial gravity. Here, we report an example of simulated fractures. The preliminary results achieved are promising and could be of practical importance in fracture characterization of carbonate reservoirs. MATLAB software has been generated for our numerical simulations.

1. Introduction

Carbonate reservoirs are of considerable interest in hydrocarbon exploration. However, they have low intrinsic porosity and permeability, but their secondary porosity either as a network of fractures or vugs provides an opportunity for geophysical characterization or it constitutes a challenging problem when compared to depositional and diagenetic reservoirs. Seismic technologies are usually helpful for enhanced reservoir delineation, but if the reservoir is deep seated, then the signal becomes low frequency, and lacks resolution.

The Earth's gravity and gravity gradient anomalies (Fig. 1) help us delineate the geological structures of economic importance such as minerals and hydrocarbon reserves. The importance of gravity gradients in exploration has become more common in the recent years due to the development of the superconducting gravity gradiometer with an accuracy of 0.02 E.U. (Eotvos Units) (Source: http://www.physics.umd.edu/GRE/SGGs.html). Recently, several researchers have highlighted the importance of tensorial gravity and offered some interpretation schemes (Kumar et al. 2012; Saad, 2000; Zhang et al. 2000).

Nagy et al. (2000) and Dubey and Tiwari (2016) have dealt with the theoretical aspects concerning gravity gradient responses of a three-dimensional isolated rectangular prism (unrotated with respect to coordinate axes) on air-earth interface (Bouguer datum). But arbitrarily oriented geometries could be a better choice in order to meet the practical situations like carbonate reservoirs with a network of fractures or vugs and sink holes.

However, tensorial gravity responses of an arbitrarily oriented rectangular parallelepiped and its projections on different borehole positions are a natural gap in knowledge. Our present effort is devoted to this aspect. The depth rules for calculating the distance of the source body using tensorial gravity measurements (in future) can be adapted from the relevant models (Nettleton, 1940). Rim and Li (2012) have studied the feasibility of imaging density variations away from boreholes using gravity gradient measurements in a single borehole. In addition, they deduced that as few as two independent gravity gradient measurements in a single borehole could be used to locate the isolated anomalous density bodies.

Borehole Tensorial gravity modelling

Here, we report a transform for building up the tensorial gravity forward responses of an arbitrarily oriented parallelepiped both at air-earth interface and in the subsurface. We consider forward responses of a rectangular parallelepiped in our synthetic experiments, especially in terms of tensorial gravity logs in different boreholes with respect to the source body and their analysis for model parameters. In such an effort, we integrated both the surface and vertical tensorial gravity profiles. We report the preliminary results of such simulation studies, which include fractures. Matlab software is generated for both modelling and analysis. Results achieved can be of practical relevance in fracture characterization of carbonate reservoirs.

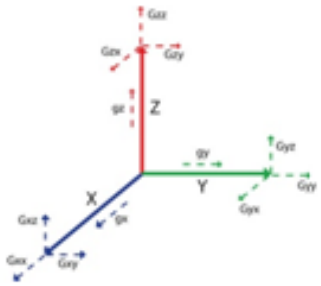

Fig. 1 A schematic diagram for full tensorial gravity measurements

Theory

We propose a simple but novel coordinate transformation for obtaining the gravity and tensorial gravity reponses due to anomaly source(s), which is mentioned below:

$$\begin{pmatrix} x' \\ y' \\ z' \end{pmatrix} = \begin{pmatrix} 1 & 0 & 0 \\ 0 & \cos u & \sin u \\ 0 & -\sin u & \cos u \end{pmatrix} * \begin{pmatrix} \cos v & 0 & \sin v \\ 0 & 1 & 0 \\ -\sin v & 0 & \cos v \end{pmatrix} * \begin{pmatrix} \cos w & \sin w & 0 \\ -\sin w & \cos w & 0 \\ 0 & 0 & 1 \end{pmatrix} * \begin{pmatrix} x \\ y \\ z \end{pmatrix} (1)$$

where P(x, y, z) represent the original coordinates of the body before any rotation has taken place. Q(x', y', z') represent the coordinates of the body after it being rotated using angles u, v & w. Angle "u" represents the rotation of the body in a plane perpendicular to the x-axis, "v" and "w" are respectively for y- and z-axes.

The forward gravity and its gradient expressions for rectangular parallelepiped are already available in literature (Nagy et al. 2000; Dubey and Tiwari, 2016).

Numerical Experiments and Results

Figure 2 deals with the model and its responses in XY and YZ- planes for a rectangular parallelepiped (unrotated). Interpreted parameters are included in Table 1.

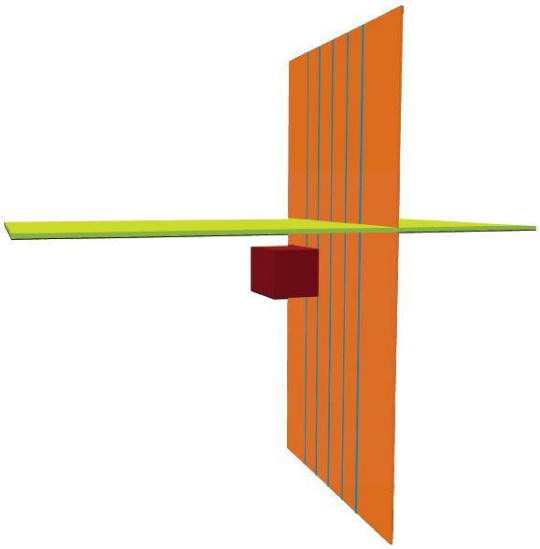

Figure 2a) A rectangular parallelepiped (in red) model (unrotated) in the subsurface with the planes, where gravity gradient responses are computed. The XY- (yellow) and YZ- (orange) plane with marked boreholes in blue colour are shown.

Borehole Tensorial gravity modelling

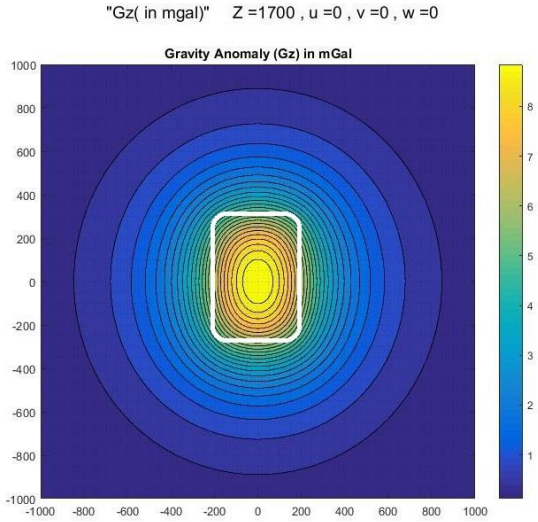

b) The vertical gravity anomaly G_z (in mgal) map over XY-plane at a depth of Z = 1700m (100m above the anomaly source surface). The outline of the body is shown in white colour.

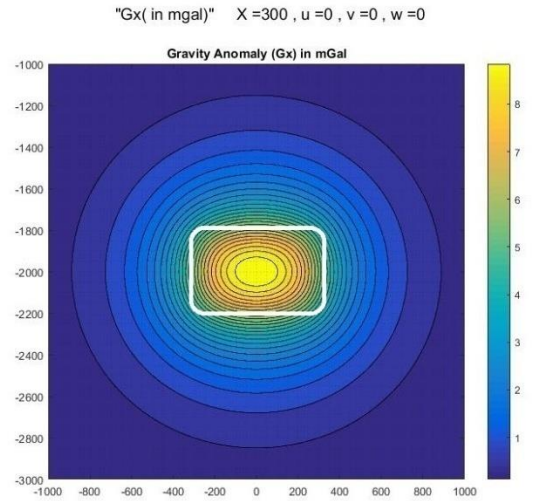

c) The vertical gravity anomaly G_z (in mgal) of an unrotated rectangular parallelepiped, observed from the YZ-plane at the distance of X = 300m from the body centre (100m from the surface). In addition, the outline of the body is shown in white colour.

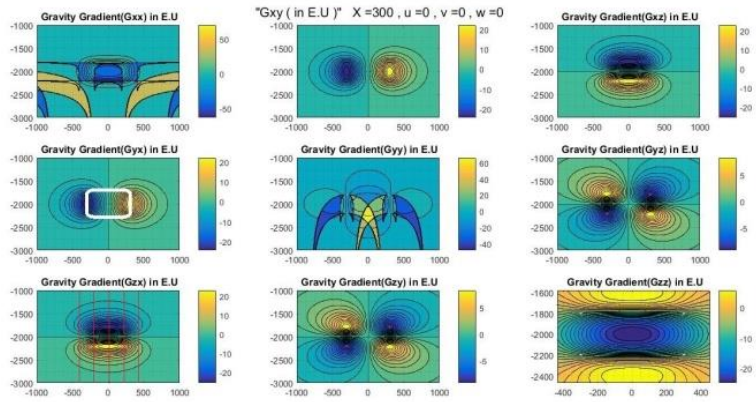

d) The tensorial gravity responses (in E.U) of an unrotated rectangular parallelepiped generated on the YZ-plane at a distance of X = 300m. Five borehole positions (red vertical lines) are shown in G_{zx} component and the outline of the body (white colour) is shown in the G_{yx} component.

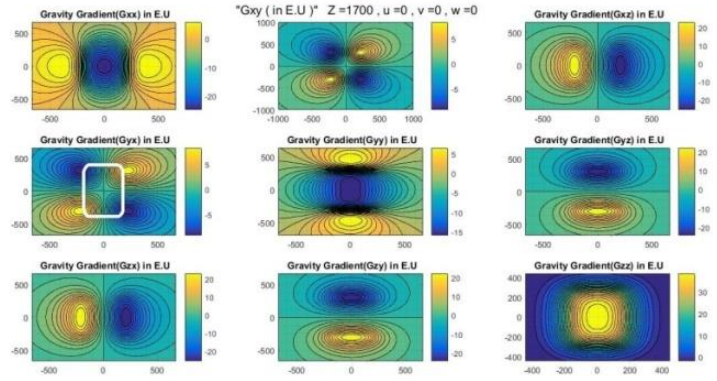

e) The tensorial gravity responses (in E.U) of an unrotated rectangular parallelepiped generated on the XY-plane at a depth of Z = 1700m. The outline of the body (white colour) is shown in the G_{yx} component.

Table 1: Estimated distances of borehole from target body using depth rules (Nettleton, 1940) for tensorial gravity log responses. These estimates refer to the unrotated rectangular parallelepiped (u = v = w = 0).

Borehole Tensorial gravity modelling

Boreholes			Factor			Cal. Dist(m)	Act. Dist(m)	Error (%)
No rotation Rectangular Parallelepiped								
300, 400	grav	Z = 1.345 * $X_{1/2}$	1.345	Gz	18	484	500	3.16
	grad	Z = 1.897 * $X_{1/2}$	1.897	Txy	13	493	500	1.36
	curv	Z = 1.454 * X_0	1.454	Tzz	16	465	500	6.94
300, 200	grav	Z = 1.345 * $X_{1/2}$	1.345	Gz	13.75	370	360	2.74
	grad	Z = 1.897 * $X_{1/2}$	1.897	Txy	12.5	474	360	31.74
	curv	Z = 1.454 * X_0	1.454	Tzz	12.5	364	360	0.97
300, 0	grav	Z = 1.345 * $X_{1/2}$	1.345	Gz	24	646	670	3.64
	grad	Z = 1.897 * $X_{1/2}$	1.897	Txy	17.5	664	670	0.90
	curv	Z = 1.454 * X_0	1.454	Tzz	22	640	670	4.51
300, -200	grav	Z = 1.345 * $X_{1/2}$	1.345	Gz	13	350	360	2.86
	grad	Z = 1.897 * $X_{1/2}$	1.897	Txy	12	455	360	26.47
	curv	Z = 1.454 * X_0	1.454	Tzz	12.5	364	360	0.97
300, -400	grav	Z = 1.345 * $X_{1/2}$	1.345	Gz	18.5	498	500	0.47
	grad	Z = 1.897 * $X_{1/2}$	1.897	Txy	13	493	500	1.36
	curv	Z = 1.454 * X_0	1.454	Tzz	17	494	500	1.13

The depth rules are suitably modified here by considering respective depth rules for point and line sources respectively.

Arbitrarily oriented Rectangular Parallelepiped

In Fig. 3**,** we include the results of an arbitrarily oriented rectangular Parallelepiped. Interpreted results are included in Table 2.

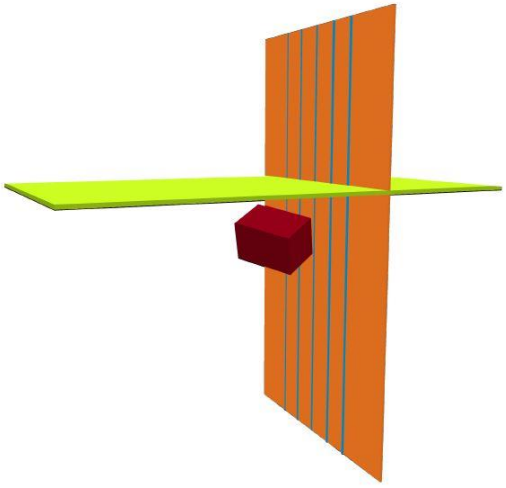

Fig. 3 A rotated rectangular parallelepiped (red) in the subsurface, and the planes of calculating gravity gradient responses (XY- (yellow) and YZ- (orange) plane) and boreholes (blue profiles)

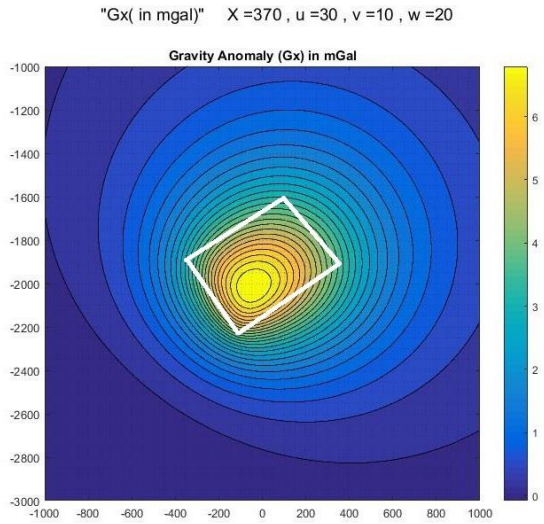

a) The vertical gravity anomaly Gz (in mgal) of rotated rectangular parallelepiped (u = 30, v = 10, w = 20), generated on the XY-plane at a depth of Z = 1630m (170m above the body surface). In addition, the outline of the body is shown in white colour.

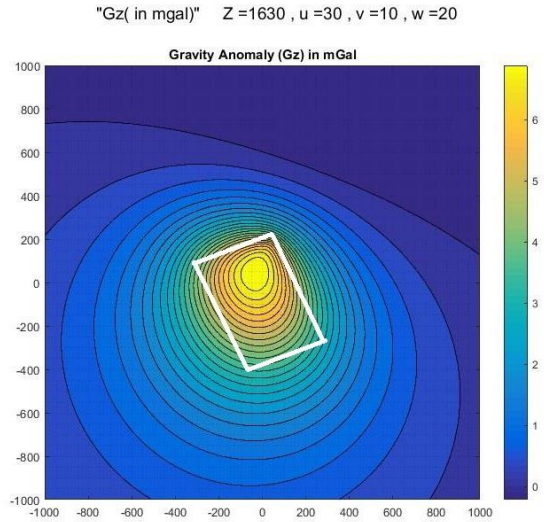

b) The vertical gravity anomaly Gz (in mgal) of a rotated rectangular parallelepiped (u = 30, v = 10, w = 20), generated on the YZ-plane at a distance of X = 370m (170m from the body surface). In addition, the outline of the body is shown in white colour.

Borehole Tensorial gravity modelling

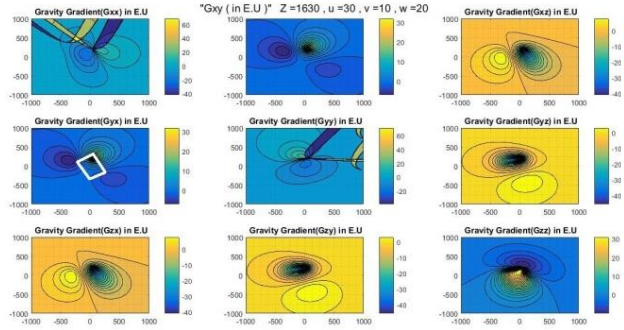

c) Tensorial gravity in XY-plane for rotated rectangular parallelepiped (u = 30, v = 10, w = 20), generated on the XY-plane at a depth of Z = 1630m (170m above the body surface). In addition, the outline of the body is shown in white colour for G_{yx} component.

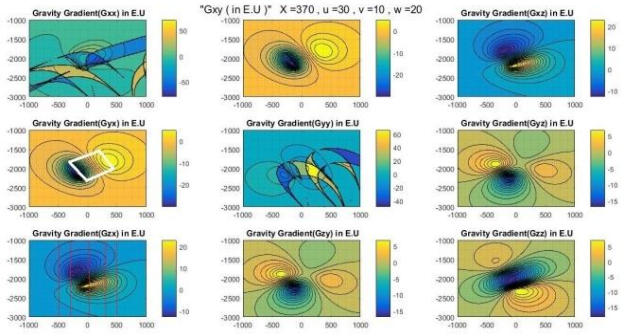

d) Tensorial gravity in YZ-Plane for rotated rectangular parallelepiped (u = 30, v = 10, w = 20), generated on the XY-plane at a depth of Z = 1630m. The five borehole positions are shown in G_{zx} plot.

Table 2: Estimated distances of borehole from target body using depth rules (Nettleton, 1940) for tensorial gravity log responses. These estimates refer to the rotated rectangular parallelepiped (u = 30, v = 10, w = 20). The depth rules are suitably modified here by considering respective depth rules for point and line sources respectively.

For a body, X 30, Y 10, Z 20	After fitting		X 200	Y 300	Z 300			
Boreholes			Factor		Diff	Cal. Dist(m)	Act. Dist(m)	Error (%)
370, 500	grav	Z = 1.345 * $X_{1/2}$	1.345	Gz	45	605	522	15.95
	grad	Z = 1.897 * $X_{1/2}$	1.897	Txy	34	645	522	23.56
	curv	Z = 1.454 * X_0	1.454	Tzz	35	509	522	2.51
370, 300	grav	Z = 1.345 * $X_{1/2}$	1.345	Gz	36	484	476	1.72
	grad	Z = 1.897 * $X_{1/2}$	1.897	Txy	30	569	476	19.56
	curv	Z = 1.454 * X_0	1.454	Tzz	28	407	476	14.47
370, 0	grav	Z = 1.345 * $X_{1/2}$	1.345	Gz	31	417	370	12.69
	grad	Z = 1.897 * $X_{1/2}$	1.897	Txy	21	398	370	7.67
	curv	Z = 1.454 * X_0	1.454	Tzz	21	305	370	17.48
370, -300	grav	Z = 1.345 * $X_{1/2}$	1.345	Gz	32	430	476	9.58
	grad	Z = 1.897 * $X_{1/2}$	1.897	Txy	22	417	476	12.32
	curv	Z = 1.454 * X_0	1.454	Tzz	30	436	476	8.36
370, -500	grav	Z = 1.345 * $X_{1/2}$	1.345	Gz	43	578	522	10.80
	grad	Z = 1.897 * $X_{1/2}$	1.897	Txy	29	550	522	5.39
	curv	Z = 1.454 * X_0	1.454	Tzz	37	538	522	3.06

Double Fracture Model

Figure 4 is devoted to two simulated fractures and the respective borehole tensorial gravity logs are shown in Fig. 4. Tables 3 and 4 respectively outline the results for two simulated fractures in Fig. 4.

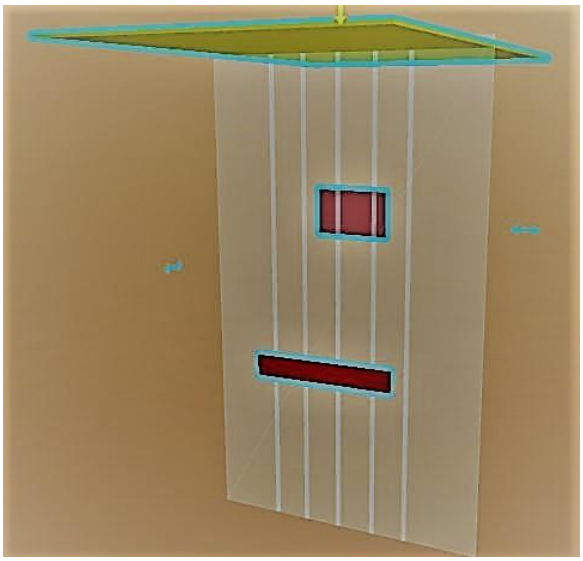

Fig. 4 An unrotated rectangular parallelepipeds (red) in the subsurface, and the planes of calculating gravity gradient responses (XY- (yellow) and YZ- (orange) plane) and boreholes (white profiles)

Borehole Tensorial gravity modelling

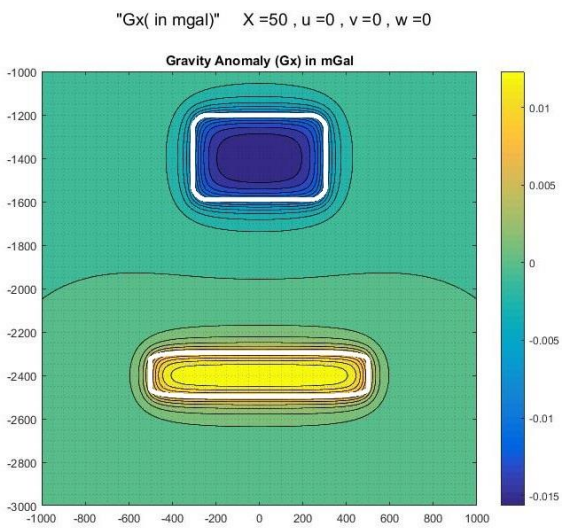

a) The vertical gravity anomaly G_x (in mgal) of the two fractures, generated on the YZ-plane at a distance of X = 50m. In addition, the outline of the fractures is shown in white colour.

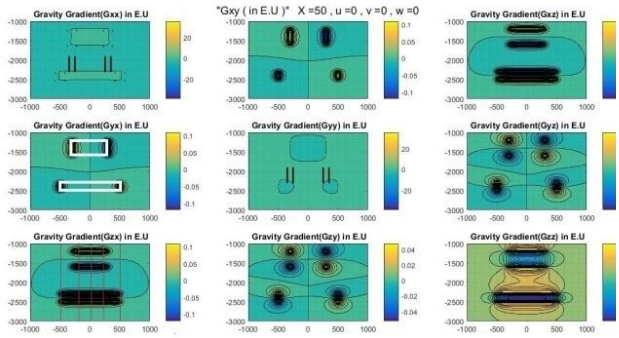

b) The tensorial gravity responses (in E.U) of the two fractures generated on the YZ-plane at a distance of X = 50m. Five borehole positions (red vertical lines) are shown in G_{zx} component and the outline of the fractures (white colour) is shown in the G_{yx} component.

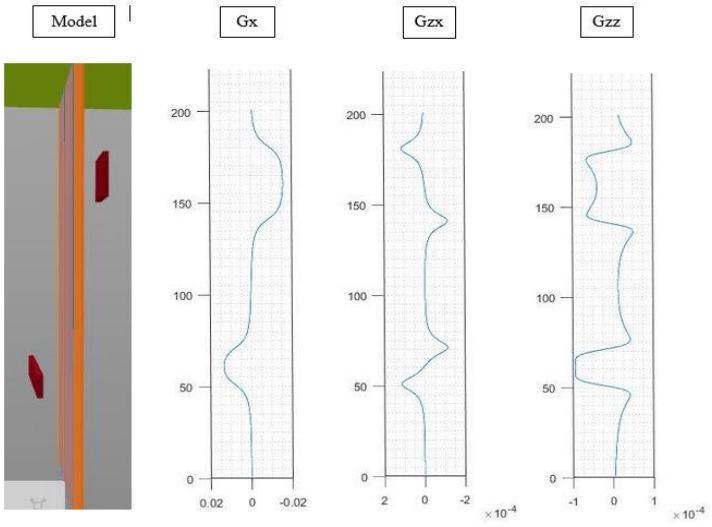

c) Gravity and its gradient logs for two simulated fractures

Table 3 Estimated width and edge detection of the target body using the for tensorial gravity log responses acquired from the boreholes. These estimates refer to the simulated fracture 1 shown in Fig. 3

For Fracture - 1		Fracture simulation (side view)					
Boreholes			Edge 1	Edge 2	Cal. Width	Act. Width	Error (%)
50,500	grav	Gz	1190	1620	430	400	7.50
	grad	Gxy	1205	1610	405	400	1.25
	curv	Gzz	1200	1605	405	400	1.25
50,200	grav	Gz	1200	1625	425	400	6.25
	grad	Gxy	1190	1605	415	400	3.75
	curv	Gzz	1195	1600	405	400	1.25
50,0	grav	Gz	1190	1610	420	400	5.00
	grad	Gxy	1197	1605	408	400	2.00
	curv	Gzz	1200	1602	402	400	0.50
50,-200	grav	Gz	1190	1615	425	400	6.25
	grad	Gxy	1200	1615	415	400	3.75
	curv	Gzz	1195	1605	410	400	2.50
50,-500	grav	Gz	1185	1610	425	400	6.25
	grad	Gxy	1190	1605	415	400	3.75
	curv	Gzz	1200	1605	405	400	1.25

Table 4 Estimated width and edge detection of the target body using the for tensorial gravity log responses acquired from the boreholes. These estimates refer to the simulated fracture 2 shown in Fig.3

Borehole Tensorial gravity modelling

For Fracture - 2		Fracture simulation (side view)					
Boreholes			Edge 1	Edge 2	Cal. Width	Act. Width	Error (%)
50,500	grav	Gz	2290	2510	220	200	10.00
	grad	Gxy	2290	2507	217	200	8.50
	curv	Gzz	2295	2502	207	200	3.50
50,200	grav	Gz	2295	2510	215	200	7.50
	grad	Gxy	2297	2505	208	200	4.00
	curv	Gzz	2297	2505	208	200	4.00
50,0	grav	Gz	2297	2502	205	200	2.50
	grad	Gxy	2295	2502	207	200	3.50
	curv	Gzz	2300	2505	205	200	2.50
50,-200	grav	Gz	2290	2505	215	200	7.50
	grad	Gxy	2295	2500	205	200	2.50
	curv	Gzz	2297	2500	203	200	1.50
50,-500	grav	Gz	2290	2507	217	200	8.50
	grad	Gxy	2295	2505	210	200	5.00
	curv	Gzz	2292	2500	208	200	4.00

Summary and Conclusions

1. For delineating the deep-seated hydrocarbon bearing carbonate reservoirs, conventional surface seismic face problems of low resolution and signal attenuation.
2. As conventional logging sensors have limited radius of investigation, tensorial gravity could be another option. Our theoretical formulations for synthetic tensorial gravity responses for an arbitrarily oriented rectangular parallelepiped utilize the novel coordinate transformation in 3-D space. We demonstrate the practical utility of borehole version of tensorial gravity measurements.

Further Perspectives

The estimation of attitude of parallelepiped in space, its dimensions and density is under way. Natural extension of our results to magnetic case is also under active consideration. The case of a multitude of fractures, in different orientations can also be considered for future extension of this modelling. In near future, the development of borehole gravity gradiometer sensor(s) holds the promise for characterizing carbonate reservoirs that are presently beyond the reach of conventional logging sensors.

References

Dubey, C.P., and V.M. Tiwari, 2016, Computation of gravity field and its gradient: Some applications: Computers & Geosciences, **88**, 83-96.

Kumar, M., A.K. Khanna, and Rahul Dasgupta, 2012, Gravity gradiometry: potent potential field method: 9th Biennial International Conference & Exposition on Petroleum Geophysics.

Nagy, D., G. Rapp and J. Bendek, 2000, The gravitational potential and its derivatives for the prism: Journal of Geodesy, **74**, 552-560.

Nettleton, L.L., 1940, Geophysical prospecting for oil: McGraw-Hill Book CO., Inc.

Rim, H., and Y. Li, 2012, Single-hole imaging using borehole gravity gradiometry: Geophysics, **77**, no. 5, G67-G76.

Saad, A.H., 2006, Understanding gravity gradients – a tutorial: The Leading Edge, **25**, no.8, 942-949.

Zhang, C., M. F. Mushayandebvu, A. B. Reid, J. D. Fairhead, and M. E. Odegard, 2000, Euler deconvolution of gravity tensor gradient data: Geophysics, **65**, 512–520.